

High-Resolution Structures of Large Ribosomal Subunits from Mesophilic Eubacteria and Halophilic Archaea at Various Functional States

Ada Yonath*

Department of Structural Biology, Weizmann Inst. of Science, Rehovot, Israel and Max-Planck-Research Unit for Ribosomal Structure, Hamburg



Abstract: Structural analysis of the recently determined high resolution structures of the small and the large ribosomal subunits from three bacterial sources, assisted by the medium resolution structure of a complex of the entire ribosome with three tRNAs, led to a quantum jump in our understanding of the process of the translation of the genetic code into proteins. Results of these studies highlighted dynamic aspects of protein biosynthesis; illuminated the modes of action of several antibiotics; indicated strategies adopted by ribosomes for maximizing their functional activity and revealed a wealth of architectural elements, including long tails of proteins penetrating the particle's cores and stabilizing the intricate folds of the RNA chains. Binding of substrate analogues showed that the decoding and the peptide-bond formation are accomplished mainly by RNA. However, several proteins may be functionally relevant in directing the mRNA and in mediating the proper orientation of the tRNA molecules within the ribosomal rRNA frame. Elements involved in intersubunit contacts or in substrate binding are inherently flexible, but maintain well-ordered characteristic conformations in unbound particles. The ribosomes utilize this conformational variability for optimizing their efficiency and minimizing non-productive interactions, hence disorder of functionally relevant features may be linked to less active conformations or to far from physiological conditions. Clinically relevant antibiotics bind almost exclusively to rRNA. In the small subunit they affect the decoding accuracy or limit conformational mobility and in the large subunit they either interfere with substrate binding, by interacting with components of the peptidyl transferase cavity, or hinder the progression of the growing peptide chain.

1. INTRODUCTION

Ribosomes are the universal cellular organelles catalyzing the sequential polymerization of amino acids according to the genetic blueprint, encoded in the mRNA. They are built of two subunits that associate for performing this task. The larger subunit creates the peptide bonds and provides the path along which the nascent protein chain emerges out of the ribosome. The smaller subunit has key roles in the initiation of the process; in decoding the genetic message; in discriminating against cognate, non- and near-cognate aminoacylated tRNA molecules; in controlling the fidelity of codon-anti-codon interactions and in mRNA/tRNA translocation. The prokaryotic ribosomal subunit (called 30S) has a molecular weight of 8.5×10^5 Dalton and contains one RNA chain of over 1500 nucleotides and 20 proteins. The prokaryotic large ribosomal subunit (called 50S) is of molecular weight 1.5×10^6 Dalton and contains two RNA chains with a total of about 3000 nucleotides and around 35 proteins. The small ribosomal subunit (called 30S) has a molecular weight of 8.5×10^5 Dalton and contains one RNA chain of over 1500 nucleotides and around 20 proteins.

Over two decade ago we initialized a long and demanding search for the determination of the three-dimensional structure of the ribosome by X-ray crystallography.

The key to high resolution data was to crystallize homogenous preparations under conditions similar to their *in-situ* environments or to induce a selected conformation after the crystals were formed. Relatively robust ribosomal particles were chosen, assuming that they would deteriorate less during preparation and therefore provide more homogenous starting materials for crystallization. The first crystals that yielded preliminary crystallographic information were grown from of the large subunit from *Bacillus stearothermophilus* [1]. It took a few years until we identified an additional source, the large ribosomal subunit from *Haloarcula marismortui* (H50S) [3] that later yielded high resolution diffraction [4,5]. A few additional years were needed for obtaining crystals of the small subunit from *Thermus thermophilus* (T30S) [6,7] and only recently we crystallized the large subunits from a mesophilic source, *Deinococcus radiodurans*, D50S, which was shown to yield quality diffraction at high resolution [8]. An alternative approach was to design complexes containing ribosomes at defined functional stages, such as of the entire ribosome with two tRNA molecules and a short mRNA analogue [9].

All ribosomal crystals present challenging technical problems, resulting from their enormous size; their complexity; their natural tendency to deteriorate and disintegrate; their internal flexibility and their sensitivity to irradiation. For minimizing the harm caused by the latter, we pioneered crystallographic data collection at cryogenic temperature [10]. This, together with the dramatic advances of the X-ray sources, namely the installation of third generation synchrotrons equipped with state-of-the-art

*Address correspondence to this author at the Department of Structural Biology, Weizmann Institute, Rehovot, 76100, Israel; Tel: -972-8-9343028, Fax: -972-8-9344154; E-mail: ada.yonath@weizmann.ac.il

detectors, and the increased sophistication in phasing, enabled us, as well as others, to handle most of the technical problems. Consequently, structures of ribosomal particles [7,11-13] and their complexes with substrate analogues and antibiotics that bind to ribosomes [13-20] are currently emerging with an impressive speed. Among them, the structures of the large ribosomal subunit from two phylogenetic kingdoms, eubacteria and archaea, were determined. This chapter compares these two structures, focusing on mobility, flexibility, and functional relevance.

H. marismortui, the bacterium that lives in the Dead Sea, the lake with the highest salinity in the world, was the source of the first ribosomal crystals that diffract to high resolution. This bacterium not only withstands the high salinity of the lake (~4 M NaCl) and the elevated temperatures of the neighborhood, it is dependent on extreme conditions. Furthermore, it accumulates enormous amounts of KCl, although the lake contains only minute amounts of this salt (Table 1 and in [22]). The reasons for the potassium intake are, most probably, not related to the ribosome function. Yet, the ribosomes of this bacterium adapted to the bacterial *in-situ* environment, and it was found that the ribosomal functional activity is directly linked to the concentration of potassium ions (Table 2 and in [3]).

Lowering the salt concentration causes first the loss on the functional activity of *H. marismortui* ribosomes, and then leads to gradual disintegration of the ribosomal particles. This process is reversible, as long as all the components of the halophilic ribosomes are still held together, strongly or loosely. Thus, the functional activity of the ribosomes can be recovered by increasing the KCl concentration. We took advantage of this property for designing the crystallization procedure, since we found that at ~3M KCl the crystals obtained from H50S are of low quality. According to this procedure crystallization is performed at around the lowest potassium concentration required for maintaining the

Table 1. The Concentration of Ions Within the Cells of *H. marismortui* (Based on [15])

	Early log	Late log	Stationary
K in cells:	3.7-5.0 M	3.7-4.0 M	3.7-4.0 M
Na in cells:	1.2-3.0 M	1.6-2.1 M	0.5-0.7 M

Table 2. The Correlation Between KCl Concentration and the Functional Activity of the Ribosomes from *H. marismortui* (Based on [3])

	3M KCl	2.5 N KCl	2 M KCl	1.5 M KCl
Activity	100%	90%	50%	20%

* Activity was measured in the presence of KCl (as shown) together with 0.5-1.5 M ammonium chloride, > 10 mM magnesium chloride and up to 1.5 M NaCl. It is defined as the fraction of the amino acids that were incorporated into growing protein chains, compared to the activity at 3 M KCl (using natural or man-made mRNA).

integrity of the ribosomal subunits and once the crystals grow they are transferred to solutions mimicking the *in-situ* conditions, namely around 3 M KCl. As the crystals obtained a very high amount of continuous solvent regions [23,24], the crystallized particles are re-arranged within the crystals into their active conformation and regain their full functional activity.

The high potassium concentration within these crystals (2.8-3.0 M) caused severe problems in the course of structure determination [23,24]. The combination of extensive non-isomorphism, apparent twinning, high radiation sensitivity, unstable cell constants, non-uniform mosaic spread and uneven reflection shape, hampered the collection of data usable for structure determination. As these problems became less tolerable at higher resolution, the structure determination under close to physiological conditions stalled at resolutions lower than 5 Å [23-26].

Drastic reduction of the salt concentration in the stabilization solution of the crystals of H50S and the exchange of the main cellular component, KCl (~3M) by NaCl (~1.5M), yielded improved diffraction and led to a structure at 2.4 Å resolution [9]. These conditions allow for low activity in protein biosynthesis [3] and for binding of compounds believed to be substrate analogues, such as CCdA-phosphate-puromycin [14]. These binding studies indicated the location of the site where the peptide bond is formed. However, the mechanism of the peptidyl-transferase activity is still not well understood [27,28], and it was shown that in contrast to the strict requirements for binding of antibiotics, all nucleotides that seem to be crucial for the catalytic activity in the proposed mechanism, could be mutated with little or no effect on peptide bond formation, *in vitro* [29] and *in-vivo* [30].

The 2.4 Å model of H50S obtained under the modified salt conditions [11] does not contain several features, all known to be involved in key functional aspects of the biosynthetic process. Among them are the lateral protuberances that create the most prominent features in the typical shape of the large subunit, the L1 stalk (H76-H78 with their bound protein L1) and the L7/L12 stalks (H43-H44 and their bound proteins L10 and L12). Proteins L12 and L10 are involved in the contacts with the translocating components as well as with factor-dependent GTPase activity [31]. Protein L11 is involved in elongation factor activities [32], and the absence of protein L1 has a negative effect on the rate of protein synthesis [33,34]. All four proteins are known to be rather flexible [31,35-37] and to be held loosely by the core of the large subunit [37,38]. Interestingly, they match the list of proteins that we detached selectively from halophilic ribosomes [37,38] under conditions similar to those used for obtaining the high-resolution structure of H50S. In addition, almost all the structural features known to be involved in the non-catalytic functional aspects of protein biosynthesis were found to be disordered in the 2.4 Å structure of H50S [11]. These include the RNA helical elements that form the intersubunit bridge called "the A-site finger" (H38), the bridge reaching the decoding center and interacting with the tRNA molecules (H69); and the central loop of protein L5 that forms the only

intersubunit bridge that is made solely of proteins (together with protein S13 from the small subunit).

The findings that almost all functionally active features are disordered features in high resolution map of H50S [11] stimulated the notion that the structural elements that interact with the small subunit or with tRNA, are generally disordered in the unbound large subunit, and become stabilized in the 70S [17]. However, it is conceivable that part of the disorder is linked to their lower functional activity, since the structure of H50S was determined under far from physiological conditions. In order to shed light on this fundamental point, we initiated crystallographic studies on the large ribosomal subunit from *D. radiodurans*, an extremely robust gram-positive eubacterium with a ribosome that shares extensive similarity the ribosomes of *E. coli* and *T. thermophilus* [39].

D. radiodurans was originally identified as a contaminant of irradiated canned meat, and later isolated from environments that are either very rich or extremely poor in organic nutrients, ranging from soil and animal feces to weathered granite in a dry Antarctic valley, room dust, wastes of atomic-piles and irradiated medical instruments. It also is the organism with the highest level of radiation-resistance currently known. It survives under conditions that cause DNA damage, such as hydrogen peroxide, and ionizing or ultraviolet radiation. It contains systems for DNA repair, DNA damage export, desiccation, starvation recovery and genetic redundancy. Well diffracting crystals of the large ribosomal subunit of *D. radiodurans* (D50S) and of its complexes with many antibiotics and substrate analogues were grown and kept under conditions almost identical to those optimized for testing their biological activity [8]. These crystals were found to provide an excellent system to investigate the peptide bond formation, to gain more insight into functional flexibility, and to extend the information of antibiotics binding towards rational drug design [21].

2. COMPARATIVE STUDIES ON LARGE RIBOSOMAL SUBUNITS

The availability of two high resolution crystal structures of unbound large ribosomal subunits, the archaeal H50S and eubacterial D50S, as well as a lower resolution structure of T50S within the T70S ribosome, provide a unique tool for comparative studies. In the particular case of H50S and D50S, such comparison should shed light on the correlation between the structure, the function, and the environment, as well as on phylogenetic aspects. We found that the structure of D50S is significantly more ordered than that of H50S. Thus, most of the features that are disordered in H50S [11] are resolved in T70S [18] and in D50S (Fig. 1a and in 9). These include the inter-subunit bridges, H38, H69 and the middle loop of protein L5; the L1 arm (helices H76-H78) and the GTPase center (helices H42-H44 and protein L11). All show defined orientations that differ from those seen in the 5.5 Å structure of the 70S ribosome complex [18], manifesting their inherent flexibility and rationalizing their contribution in the functional tasks assigned for them.

The gross similarity of the rRNA fold of D50S to the available 50S structures allowed superposition of the model of D50S onto that of the 2.4 Å structure of H50S [11] and of the 50S subunit within the 5.5 Å structure of the T70S ribosome [18]. We found that the RNA fold and the overall protein distribution are rather similar in the three structures, but detected significant structural differences even within the conserved regions, which cannot be explained solely by expected phylogenetic variations. In contrast to the significant similarity between the RNA fold of D50S and H50S, the proteins show remarkable differences, even when sharing homology with their counterparts in H50S. In addition, D50S contains several proteins that have no counterparts in H50S. We detected RNA segments replacing proteins and vice versa. Of structural interest is a three domains protein (CTC), alongside with an extended alpha helical protein (L20) and two Zn-finger proteins (L32 and L36). Analysis of the general modes of the RNA-protein interactions within D50S did not reveal striking differences from what was reported for the other ribosomal particles. As in the 30S subunit [12,13] and in H50S [11], most of the globular domains of the D50S proteins are peripheral, located on the solvent side of the subunit, and their extensions permeate the interior of the particle, whereas the flat front side that interfaces the other subunit within the assembled ribosome, is almost free of globular domain of proteins. A few proteins, however, do not have extensions and are built of more than a single globular domain and have special positions in the D50S subunit. These are located either at the ends of functionally important protuberances (L1, L7/L12, L10, L11) or fill a gap between the central protuberance and one of the stalks (CTC).

2.1. The Peptidyl Transferase Center and its Vicinity

The peptidyl transferase activity of the ribosome has been linked to a multi branched loop in the 23S secondary structure diagram, known as the peptidyl transferase ring (PTR). From the 43 nucleotides forming the PTR, 36 are conserved in *H. marismortui* and *D. radiodurans*. Superposition of the backbone of the high resolution structures of the PTR nucleotides in the two species (11 and in PDB 1JJ2) shows a similar fold, but the orientations of some of the nucleotides show distinct differences (Fig. 1b). The main differences in the peptidyl transferase ring include translational shifts of sugar moieties that maintain co-planar bases but are pointing to different directions in the two structures, or different degrees of rotation with hardly any change in the sugar moieties. Among the PTR conserved nucleotides, A2062, C2063, C2064, U2449, A2451, C2499, U2504, G2505, and U2506 (*E. coli* numbering) display rotational or translational shifts of above 2Å. The largest rotational differences are between the base moieties of A2451 (86 degrees), A2506 (79 degrees) and U2504 (40 degrees). A2451 is the key element in the proposed peptide bond catalysis mechanism, based on the structure of H50S [11,14]. Biochemical evidence has shown the functional importance of U2504 and U2506. U2504 has been implicated in the binding of the 3' end of the aminoacyl tRNA prior to peptide bond formation [40,41] and U2506 was shown to be protected from chemical modification by P-site tRNA [42].

It is possible that the different orientations reflect the flexibility needed for the formation of the peptide bond. It is also possible, however, that the different orientations result from the differences in the functional states of the 50S subunit in the two crystal forms, consistent with the structural changes that were found to occur at distinct nucleotides of the peptidyl transferase ring upon transition between the active and inactive conformations through chemical probing with dimethyl sulfate [28]. In support of this suggestion are experiments performed over three decades ago on the *E. coli* 50S subunits [43-45], that indicated that the relative orientations of several nucleotides within the peptidyl transferase center vary upon alterations in the monovalent ion concentrations in magnitudes that are much lower than the modifications in the concentrations and types of the monovalent ions that were employed in the course of the determination of the structure of H50S [11].

In unbound D50S, as in H50S, the peptidyl transferase center seems to be clear of proteins. Protein L2, a protein often implicated in peptide bond formation, was found rather far from the peptidyl transferase center, as in H50S. One of the only proteins residing near or in the interface area of D50S, is protein L27. This protein is located at the base of the central protuberance, consistent with previous results of immuno electron microscopy, crosslinking, affinity labeling, chemical probing, mutations and footprinting (46,47 and A. Mankin, personal communication). L27 has been shown to influence the peptidyl transferase activity in *E. coli* 50S by a variety of experimental observations, including antibiotic cross-linking and a deletion mutant that shows deficiencies in the peptidyl transferase activity and impaired enzymatic binding of Phe-tRNA Phe to the A site [47,48]. It has been proposed that protein L27 plays a role in mediating the proper placement of the 3' end of the A-site tRNA at the peptidyl transferase center, by screening the negative charge of the tRNA molecules from that of the ribosomal RNA during the peptidyl transferase reaction, and influencing the interactions of the 3' end of deacylated tRNA with the ribosome after peptidyl transfer.

In D50S L27 is one of the most flexible proteins and its N-terminal tail is disordered. The parts of the protein that are well resolved, however, reach the proximity of the A- and the P-sites (Fig. 1e), consistent with the proposal that it contributes to peptide bond formation by facilitating the proper placement of the acceptor end of the A-site tRNA [47]. Careful examination of the D50S electron density map in the vicinity of L27 indicated that in the unbound D50S the disordered tail may move around rather freely, since it is located at the particle's interface. However, based on the positions of the docked tRNA molecules according to the 5.5 Å structure of the T70S/tRNA complex [17], it seems that its movements will be drastically restricted once the two subunits associate to form the functionally active 70S ribosome. These restrictions, especially in the presence of tRNA molecules in the A- and the P- sites, practically dictate that the N-terminal tail of L27 must thread its way close to the tRNA molecules in the A- and P-sites, in the direction of the designated peptidyl transferase center. It was recently suggested that the exothermic reaction of peptide bond formation is strongly dependent on proper orientation of the tRNA molecules and that the rRNA core provides the frame

for the binding of the tRNA molecules [29]. Protein L27 may be the component that enhances the accurate positioning of the tRNA molecules.

Interestingly, in H50S there is no homologous counterpart to L27. The protein that occupies the place of L27 is L21e. Contrary to L27, the tail of L21e folds backwards (Fig. 1c), towards the interior of the subunit, disabling potential contacts with the P-site tRNA. This may indicate that the halophilic ribosomes do not need a mediator for tRNA binding, perhaps because of the high salt concentration. It also may support our hypothesis that tails that are normally involved in binding factors or substrates, fold away from the action sites under less than optimal conditions.

2.2. The Nascent-Protein Exit Tunnel

More than three decades ago biochemical studies showed that the newest synthesized part of a nascent protein is masked by the ribosome [49,50]. In the mid eighties, a feature that may account for these observations was first seen as a narrow elongated region in images reconstructed at very low resolution (60 Å) in 80S ribosomes from chick embryos [51] and at 45 Å in images of 50S subunits of *Bacillus stearothermophilus* [52]. Despite the low resolution, these studies showed that this tunnel spans the large subunit from the location assumed to be the peptidyl transferase site to its lower part, and that it is about 100 Å in length and 15 Å in diameter [49], as confirmed later at high resolution in H50S [11] and in D50S [9].

The structural features building the walls of the tunnel, their chemical composition and the "nonstick" character in H50S are described in [14]. We found in D50S the same characteristics – lack of well-defined structural motifs, large patches of hydrophobic surfaces and low polarity. Despite the gross similarities, it seems that the tunnel in D50S is, in several locations, somewhat wider than that of H50S.

The opening of this tunnel, at the exit side, is located at the bottom of the particle. In D50S it is composed of components of domain III, domain I as well as several proteins, including L4, L22, L23, L24 and L29. In H50S, two proteins that do not exist in D50S, L31e L39e are also part of the lower part of the tunnel (Fig. 1d). Interestingly, the space occupied by protein L23 in D50S hosts two proteins in H50S. The halophilic L23 occupies the space taken by the globular part of L23, whereas the halophilic L39e replaces the extended loop of L23 in D50S. L39e is a small protein of an extended non-globular conformation, which penetrates into the RNA features that construct the walls of the tunnel in that region. Its extended tail is thinner than the extended loop of L23 (in D50S), therefore it penetrates deeper into the tunnel walls than the loop of L23 in D50S. L39e is present in archaea and eukaryotes, but not in eubacteria. Thus, it seems that with the increase in cellular complication, and perhaps as a consequence of the high salinity, a tighter control on the tunnel's exit was required, and two proteins (HL23 and L39e) replace a single one. So far there are no indications for a connection between this replacement and evolution. Nevertheless, a protein in this

delicate position may provide the communication path between the ribosome and other cell components, as evolving further, to act as a hook for the ribosome on the ER membrane. A high resolution structure of a eukaryotic ribosome, bound to the ER membrane, should provide an answer to these open questions.

2.3. Evolutionary Adaptation to Environmental Conditions Observed in a Single Protein

In D50S, CTC (named after a general shock protein) replaces the 5S binding proteins L25 in *E. coli* and its homologue TL5 in T50S. H50S contains neither L25 nor any of its homologues. Within the known members of the CTC protein-family, that from *D. radiodurans* is the longest. It contains 253 residues, about 150 longer than L25 from *E. coli* and 60 more than TL5 from *T. thermophilus*.

The structure of complexes of TL5 from *T. thermophilus* [53] and L25 from *E. coli* [54] with RNA fragments corresponding to their 5S RNA binding regions (40 and 18 nucleotides, respectively) were determined at high resolution. Comparisons between them showed that the structure of the N-terminal domain of TL5 is similar to that of the entire L25. CTC has three domains. The N-terminus is similar to the entire L25 and to the N-terminus of TL5. The middle domain is similar to the C-terminal domain of TL5. However, the relative orientation of the N-terminal and the middle CTC domains differs from that determined for the two domain of TL5 in isolation. The third domain of CTC, the C-terminal, is built of three long alpha helices connected by a pointed end, bearing some resemblance to structural motif seen in some small subunit proteins.

The N-terminal domain of CTC is located on the solvent side of D50S (Fig. 1e), at the presumed position of L25 in *E. coli*. The middle domain fills the space between the 5S and the L11 arm, and interacts with H38, the helix that forms the intersubunit bridge called B1 [18]. The interactions with H38 and the partial wrapping of the central protuberance (CP) of the subunit, are likely to provide additional stability, consistent with the fact that these two domains are almost identical to thermophilus substitute for protein L25 (protein TL5) in the ribosome of *T. thermophilus*.

The C-terminal domain is placed at the rim of the intersubunit interface. Docking the tRNA molecules as seen in the 5.5 Å structure of the T70S complex [18], showed that the C-terminal domain of CTC reaches the A-site, and restricts the space available for the tRNA molecules. The somewhat lower quality of the electron density map of this domain hints at its inherent flexibility, and indicates that it may serve as an A-site regulator and also have some influence on the processing of mRNA. In addition, the C-terminal domain of CTC interacts with the A-finger. This interaction, the manipulation of the binding of tRNA at the A-site, the influence on the mRNA progression and the enhanced stability of the CP caused by CTC, may be parts of the mechanisms that *D. radiodurans* developed for survival under extremely stressful conditions.

2.4. Selected Examples for Diversity

Helix H25

Helix H25 shows the greatest sequence diversity among eubacterial and halophilic large subunits. It contains 27 nucleotides in D50S and 74 in H50S. It lies on the solvent side of the subunit, and in D50S the region that is occupied by this helix in H50S, hosts two proteins, L20 and L21. These two proteins exist in many eubacterial ribosomes, but not in the large subunit of *H. marismortui* that evolved later than *D. radiodurans*. L21 has a small beta-barrel-like domain that is connected to an extended loop. L20, in contrast is built of a long alpha helical extension with hardly any globular domain. Its shape and location make L20 a perfect candidate for RNA organization. This may explain why L20 is one of the early assembly proteins, and why can it take over the role of L24 in mutants lacking the latter. The replacement of proteins by an RNA helix should be rather surprising, since in this way the ribosome could have lost two strong structure-stabilizing elements. However, in this case, regardless of what was the reason for extending helix H25 in archaea and eukaryots, this did not reduce the stabilization of this region, since protein L32e has a looped tails, sufficient in length to compensate for many of the contacts made by the tail of L20 and the loop of L21. It is therefore likely that the loop of L32e organizes the RNA environment in H50S in a fashion similar to the loop of L21 in D50S. The globular domains of protein L32e and L21 appear to be similar, and it is likely that L21 and L32e are indeed evolutionarily related. The globular domain of L32e is rotated by 180 degrees around an axis defined through its tail, and the void created in H50S by this suggested rotation of L21 to the L32e position, is occupied by the extension of H25.

Protein-Tweezers

Protein-tweezers. Among the novel protein structures of D50S are two Zn-fingers proteins, L32 and L36 that do not exist in H50S and have no replacements or counterparts. The position occupied by L32 in D50S overlaps that hosting the loop of HL22 in H50S, and in *D. radiodurans* L32 and L22 form a tweezers-like motif that seems to clamp the interactions between domains II, III and IV (junctions H26/H47, H61/H72). These two proteins interact extensively with protein L17, an additional novel protein that occupies the location of L31e in H50S, and the entire region seems to be highly stabilized. The question, still to be answered is: why, with evolution, was a protein replaced by a loop of another one, although this replacement seems to cause partial loss of stability of a well-organized structural motif?

The E-site tRNA

The E-site tRNA may interact, in D50S to the end of the extended loop of protein L31. In H50S, the region interacting with E-site RNA is provided by the extended loop of L44e. These two proteins are located at the opposite sides of the location of the E-site tRNA, yet the interactions occur at approximately the same place, utilizing their extended loops. In D50S, L33, which has no extended loop occupies the space taken by the globular domain of L44e in H50S, and the globular domains of both are rather similar. These

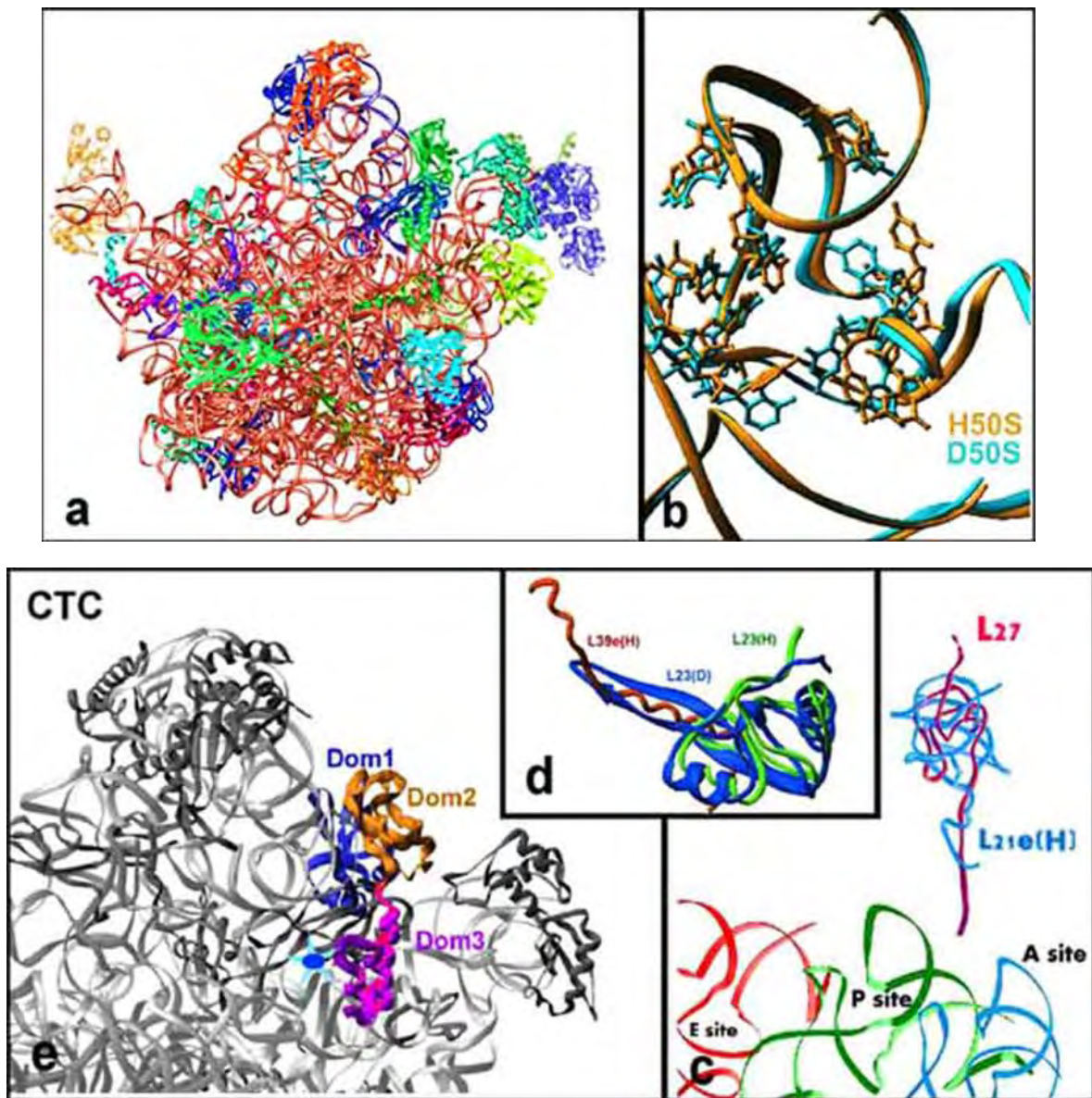


Fig. (1). (a). A crown view representation of D50S structure, shown from the side facing the small subunit within the 70S ribosome. The RNA chains are shown as ribbons (in cherry-red) and the proteins main chains in different colors. For orientation: the L12 stalk is on the right, the L1 stalk is on the left, and the central protuberance (CP), including the 5S RNA is in the middle of the upper part of the particle. (b). Superposition of the backbone of the peptidyl transfer ring of D50S on that of H50S. The nucleotides that show significant deviations are also shown. (c). Protein L27 and its location in D50S, with the resolved part of its N-terminus reaching the tRNA binding sites. For comparison, the protein that occupies the same position in H50S, L21e with its folded-backwards N-terminus, is shown. (d). Protein L23 at the opening of the tunnel in D50S and its two-proteins substitute in H50S. (e). Protein CTC is shown on the upper part of the D50S structure (gray ribbons) in the orientation of Figure 1a. The N-terminal domain is located at the solvent side, behind the central protuberance. The middle domain wraps around the central protuberance and fills the gap to L11 arm. The N-terminal domain is located at the rim of the intersubunit interface and reaches the site of docked A-site tRNA position (marked as a cyan-blue star).

complicated rearrangements may indicate that with evolution the ribosome developed different pathways in order to preserve the configurations and locations of the features involved in the peptide bond formation.

Helix H30b

Helix H30b which does not exist in D50S, is located on the solvent surface in H50S. This helix makes extensive

contacts with protein L18e, a protein that does not exist in D50S, and with the lower part of H38. Protein L18e, in turn, connects H30b to H27 and to the loop of H45 and interacts with proteins L4 and L15. This RNA-protein network seems to be rather rigid, and its strategic location may indicate that it is used as for protecting the ribosomal surface in the increasing complexity of the environment.

3. DISORDER, FLEXIBILITY AND FUNCTIONAL RELEVANCE

Most of the structural elements that are known to be involved in the non-catalytic functions of the large ribosomal subunit were found to be disordered in the 2.4 Å structure of H50. Since a large number of them were clearly detected in the 5.5 Å maps of the assembled 70S ribosome, it was suggested that these features are disordered in unbound subunits, and become stabilized once the two subunit associate and the 70S ribosome is being formed (see above and in [18]). The finding that almost all of these features are rather ordered in the unbound D50S indicates that H50S crystal structure contains features that flex more than in D50S. Biochemical, functional and electron-microscopical studies indicated that these functionally relevant features are inherently flexible. However, flexibility is not necessarily synonymous with disorder. In many cases, as in D50S and

T70S, the flexible structural elements assume several well-defined conformations, and their switch from one conformation to another is related to their functional states. It is likely that the crystallized H50S subunits underwent environmentally induced conformational changes, consistent with their storage under far from physiological conditions. This may indicate that the ribosomal strategy to avoid subunit association and substrate binding, under far from physiological conditions, is to introduce disorder in the relevant features.

3.1. The Lateral Stalks

The L1 stalk (Fig. 2) includes helices H75-H78 and protein L1. In the complex of T70S with three tRNA molecules, the L1 stalk interacts with the elbow of E-tRNA. This interaction, together with protein S7 of the small

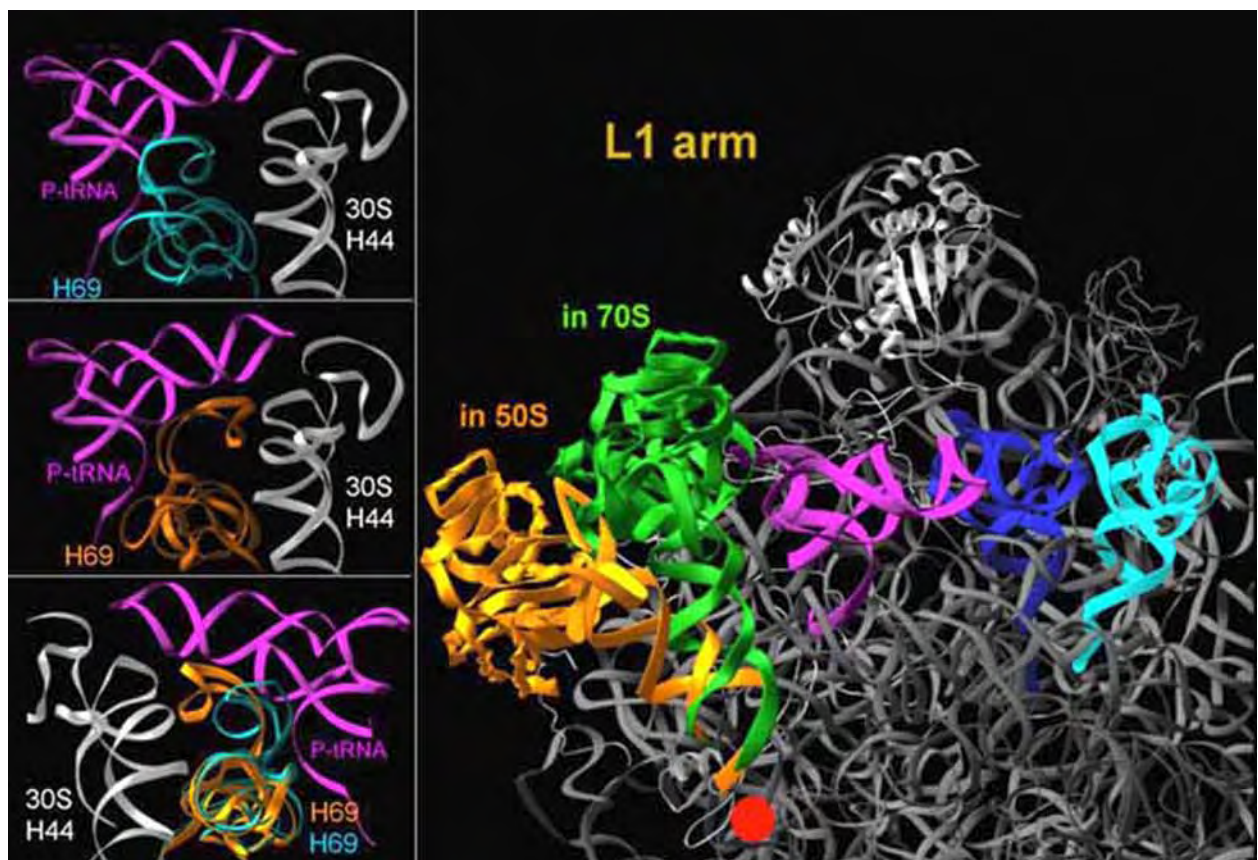


Fig. (2). Left: Bridge H69 in the unbound D50S (gold) and within the T70S ribosome (gold). For orientation, H44 (of the small subunit) and A-site tRNA (pink), are shown. D50S is rotated by 90 deg around the long axis of the view shown in figure 1 (a).

In the top and the middle it will occupy the left side of the images, and the bottom shows the opposite direction.

Top: only the unbound bridge is shown. Middle: the bridge within the 70S ribosome. Bottom: Overlay of H69 In the unbound D50S subunit (cyan) on the corresponding feature in the structure of the whole ribosome (gold). The figure indicates the proposed movement of H69 towards the decoding center of H44 (gray) in T30S.

Right: Part of the D50S structure (as gray ribbons). The L1-arm of D50S is highlighted (in gold). Also shown is the docked L1-arm of T70S (green) and protein L1 of T70S (green) and the potential location of protein L1 in D50S (yellow-gold). In T70S the L1-arm and protein L1 block the exit of the E-tRNA (magenta). Whereas, in the D50S structure, the L1-arm is rotated around a pivot point (marked by a red dot) (by ~30 deg, thus clearing the E-tRNA exit). The P-site (blue) and A-site (cyan) tRNAs are shown for orientation.

subunit, blocks the exit path for the E-tRNA. Consequently it was suggested that the release of the deacylated tRNA requires that one or both of these features move [18]. In H50S, the entire L1 arm is disordered and therefore could not be traced in the electron density map [11], an additional hint of the inherent flexibility of this feature. In D50S the RNA helices of the L1 stalk have a similar fold to that seen in T70S. However, the entire D50S L1 stalk is tilted by about 30 degrees away from its position in the T70S ribosome, so that the distance between the outermost surface points of the L1 arm in the two positions is over 30 Å (Fig. 2).

The location of protein L1 in D50S does not block the presumed exit path of the E-site tRNA. It is possible that the mobility of the L1 arm is utilized for facilitating the release of E-site tRNA. Although the orientation of the L1 arm in the 70S ribosome during the release of the E-site tRNA is still not known, the two defined orientations that have been observed indicated that movement of the L1 arm might occur during protein biosynthesis. Superposition of the structure of D50S on that of the T70S ribosome allowed the definition of a pivot point for the possible movement of the L1 arm. Similar differences found in the relative orientation of the L1 stalk have been correlated with the presence or absence of tRNA and elongation factors [55]. Hence it may be assumed that the position of the L1 stalk in the unbound D50S represents the conformational change required for the release of the E-site tRNA. Such movement may also provide an alternative explanation for the previous cryo-EM location of the E-site [56], and explain the appearance of an extra density in the vicinity of the L1 arm at the 7.5 Å cryo-EM map of the 50S subunit [54].

The second protruding region, the L7/L12 stalk, extends from the solvent side to the front surface of the large subunit, consists of H42-H44 and proteins L7/L12 and L10. In D50S the location of this stalk is somewhat shifted (by 3-4 Å) compared to its position within the 70S ribosome [18]. In the 2.4 Å structure of H50S [9] the entire L7/L12 stalk is disordered. However, a recently deposited entry to the protein data bank (PDB 1JJ2) includes coordinates of the RNA portion of the stalk (H42-H44), which shows a rotation of about 12 degrees from its position in D50S. Observing this stalk in three different orientations is consistent with the flexibility associated with its involvement in EF-G-dependent translocation. Assignment of each of the positions to a specific functional state still awaits the elucidation of high resolution structures of 70S ribosomes at the relevant states.

Protein L11, a highly conserved ribosomal protein, which is associated with the GTPase region, is located at the base of the L7/L12 stalk. L11 and the antibiotic thiostrepton bind cooperatively to a highly conserved segment of 23S RNA [32,57]. This region has been probed by several biophysical, crystallographic, NMR and electron-microscopical techniques [58-62]. The crystal structure of a complex containing L11 together with a 58 nucleotide RNA chain mimicking the RNA stretch that binds it within the E. coli 50S subunit [38] showed tight binding of the C-terminal domain of L11, but limited contacts between its N-terminal domain and the RNA. Therefore it was proposed to function as a conformational switch. In D50S the separation between

the two domains of protein L11 is somewhat larger than that observed in the isolated structures as well as in the assembled T70S [18], thus supporting the dynamic aspect of this proposal.

3.2. Flexible Intersubunit Bridges

The intersubunit bridges are the features connecting the two subunits within the assembled ribosome, namely the linkers between the two ribosomal subunits. The correct assembly of the entire ribosome from its two subunits is the key, or one of the major keys, for proteins biosynthesis, hence these bridges must be positioned accurately and point at the exact direction. Each intersubunit bridge is formed from two parts – one of the small and one of the large subunit. We found that whereas those of the small subunit are of almost the same conformation in the unbound and bound subunit, those originating from the large one are inherently flexible, and may have different conformations or assume a high level of disorder. Upon subunit association the conformations of these bridges change so that they can participate in the creation of the assembled ribosome. Thus, their structure and the nature of their conformational mobility should show how the ribosome controls its intricate assembly.

Figure (2) demonstrates a feasible sequence of events leading to the creation of the intersubunit bridge from the large subunit to the decoding center on the small one. Helix H69 that is responsible for this bridge lies in the unbound 50S subunit on the interface surface and interacts intensively with helix H70. Once the initiation complex that includes the small subunit and tRNA at the P-site approaches the large subunit, the tRNA pushes helix H69 towards the decoding center, and the intersubunit bridge is formed.

The orientation of H69 with its universally conserved stem-loop in D50S is somewhat different than that seen in T70S. Both lie on the surface of the intersubunit interface, but in the 70S ribosome it stretches towards the small subunit, whereas in the free 50S it makes more contacts with the large subunit (H71), so that the distance between the tips of their stem-loops is about 13.5 Å. Comparison of the two orientations of H69 (Fig. 2) indicates that a small rotation of H69 in the free 50S subunit is sufficient for turning this helix into bridging position, so that it can interact with the small subunit near the decoding center in Helix H44. In this position H69 can also contact the A- and P-site tRNA molecules, and be proximal to elongation factor EF-G and in the post-translocation state [18]. Although it seems that H69 undergoes only subtle conformational rearrangements between the free and the bound orientations, it is clear that the displacement and the rotation of a massive helix like H69 require a high level of inherent flexibility. This may explain why in the 2.4 Å structure of H50S, which was determined at far from physiological conditions, H69 is disordered [11].

Protein L5, together with S13 that is located in the head of the small subunit, form the only intersubunit bridge (B1b) that is constructed solely from proteins [18]. The entire domain of L5 that is involved in this bridge is missing in H50S and resolved in D50S, having a structure similar to

that observed in crystals of isolated protein S5 [63]. Additional RNA features that are involved in intersubunit contacts are helices H62, H64, H69 and the lateral arm composed of H68-H71. All are present in the D50S structure in a fashion that allows their interactions with the small subunit, and have similar conformations to those seen in T70S [18].

Proteins L14 and L19 form an extended inter-protein beta sheet, composed of two beta-hairpin loops of L14 and two of L19 (Fig. 2). In H50S, there is no L19, but L24e, although different in shape and smaller in size, is located at the same position and forms a similar beta sheet element. Both L14 and L19 are directly involved in intersubunit bridges. L19 is known to make contacts with the penultimate stem of the small subunit, at bridge B6. L14 contacts helix H14 of the 16S RNA to form bridge B8. It is likely, therefore, that the structural element produced by L14 and its counterpart (L19 or L24e) has functional relevance in the construction of these two bridges. In D50S, these proteins together with protein L3 form one of the two intimately connected protein clusters, consistent with a large number of reported cross-links [64]. This clustering may enhance the stability of the structural features required for the intersubunit bridges.

4. ANTIBIOTICS THAT BIND TO THE LARGE SUBUNIT

Ribosomes of pathogens are a major target for natural and synthetic antibiotics. The detailed knowledge of antibiotic binding sites is the key for the understanding of the mechanisms of drug action as well as an excellent tool for studying ribosomal function. *D. radiodurans* are sensitive to all clinically important antibiotics agents that target ribosomes, contrary to halophilic ribosomes that show significant resistance to antibiotics [65].

Difference electron density maps in which the 3.1 Å structure model of the 50S subunit of *D. radiodurans* [8] was used as a reference, allowed an unambiguous determination of the binding sites of the following antibiotics: chloramphenicol, clindamycin, erythromycin, clarithromycin and roxithromycin [21]. All were found to target the 50S subunit only at the peptidyl transferase cavity, and explain previous mutational and footprinting data. Each class of antibiotic among these five agents interacts exclusively with specific nucleotides, all within the so called PTR multi-branched loop of domain V of the 23S rRNA [8], and it was found that the binding of these antibiotics did not result in any significant conformational change of the peptidyl transferase cavity.

Chloramphenicol and clindamycin are known to block peptidyl transferase. In the crystal structure of the complex chloramphenicol with D50S, one of its reactive oxygens forms hydrogen bonds with C2452, which has been previously shown to be involved in chloramphenicol resistance. Its additional reactive oxygens interact with U2504, G2061 (that has been implicated in chloramphenicol resistance in rat mitochondria), U2506, G2505, U2506, and U2485 either directly or via Mg⁺⁺ ions. The binding site of the lincosamide clindamycin partially overlaps with that of

chloramphenicol. Its hydrogen bond system includes A2505, C2452 and G2505. Interestingly, neither of these antibiotics binds to A2451, the nucleotide assigned as one of the most important for the catalytic mechanism of the ribosome, based on the 2.4 Å structure of *H. marismortui*.

All three macrolides, erythromycin, clarithromycin, and roxithromycin, were located at the entrance of the protein exit tunnel, consistent with previous suggestions that they block the progression of the nascent peptide [66]. Figure (3) shows the binding site of erythromycin. Its binding site may allow the formation of 6-8 peptide bonds before the nascent protein chain reaches them. Once macrolides are bound, they reduce the diameter of the tunnel from the original 18-19 Å to less than 10 Å, and, since the space not occupied by erythromycin hosts a hydrated Mg²⁺ ion, the passage available for the nascent protein is 6-7 Å. Moreover, in order to reach this narrow passage the nascent peptide needs to progress in a diagonal direction, thus imposing further limitations on the growing protein chain. These structural results are consistent with previous biochemical findings, showing that up to eight-mers peptides can be produced by erythromycin-bound ribosomes [66].

The binding sites of all five antibiotics were found to be composed exclusively of segments of 23S rRNA at the peptidyl transferase cavity. The high affinity of the macrolides ($K_{\text{diss}} 10^{-8}$ M) to the ribosome is difficult to be explained solely by their hydrogen bonding scheme, and it is likely their binding is being further stabilized by van der Waals forces, hydrophobic interactions, and the geometry of the rRNA that tightly surrounds the macrolide molecules. Similar to the small ribosomal subunit, ribosomal proteins may affect the binding and action of ribosome-targeted antibiotics, but the primary target of these antibiotics is rRNA. The two ribosomal proteins that have been implicated in erythromycin resistance are L4 and L22. However, the closest distances of erythromycin to these proteins are 8-9 Å, distances that are too long to create meaningful chemical interactions. Therefore we suggest that the macrolides resistance acquired by mutations in these two proteins is an indirect effect, produced by a perturbation of the 23S rRNA induced by the mutated proteins, in accord with previous findings [67]. These perturbations may or may not be connected to the changes in the width of the protein exit tunnel, as proposed based on cryo electron microscopy studies, performed at low resolution [68].

These studies illuminated some of the structural principles of antibiotics action. Chloramphenicol targets mainly the A-site. It is located close to the amino acceptor group of substrate analogue CC-Puromycin [14]. It interferes with the aminoacyl moiety of the A-site tRNA, consistent with previous findings [69]. The macrolides bind close to the entrance to the protein exit tunnel, hence sterically block the progression of the nascent peptide. Clindamycin interferes with the A-site and P-site substrate binding and physically hinders the path of the growing peptide chain. In this way it bridges between the binding site of chloramphenicol and that of the macrolides. It overlaps the with both A- and P-sites, explaining its A/P hybrid nature [70]. These antibiotics could also inhibit peptidyl transferase by interfering with the proper positioning and the translocation of the tRNAs at the

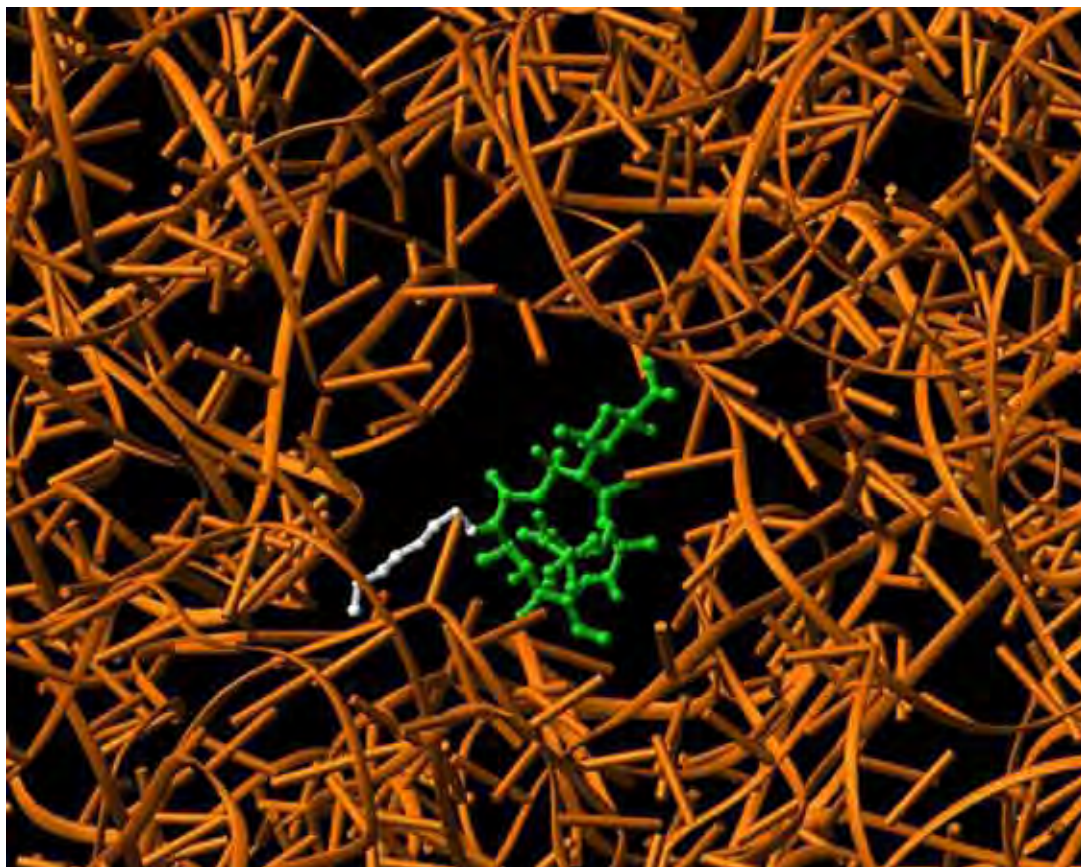


Fig. (3). The position of erythromycin (green) and roxithromycin (green + white) in D50S (only RNA is shown, in gold). The view is from the PTC into the exit tunnel.

peptidyl transferase cavity. This hindrance may be direct, as in the case of chloramphenicol, or indirect, as in the case of the three macrolides. In addition, antibiotic binding physically link regions known to be essential for the proper positioning of the aminoacyl- and peptidyl-tRNAs and thus limit the conformational flexibility needed for protein biosynthesis.

The binding sites of these antibiotics have some overlapping nucleotides, explaining why clindamycin and macrolides bind competitively to the ribosome and why most RNA mutations conferring resistance to macrolides also confer resistance to lincosamides (reviewed in [66]). The common nucleotides targeted by antibiotics may be considered as essential to peptide bond formation. Hence, the information derived from the overlapping binding sites may indicate how to create powerful antibiotics combinations and how to design antibiotics of a higher stability.

The interactions of these antibiotics together with the lack of major conformational changes occurring upon antibiotic binding, favor the suggestion that the peptidyl transferase center serves as a template for proper positioning of the aminoacyl- and the peptidyl-tRNA molecule to allow for spontaneous creation of peptide bonds [29]. The ribosomal components that may construct the frame holding

the tRNA molecules and contribute to the correct accurate positioning of the tRNA molecules, such as the PTR and protein L27, are discussed above and shown in Figure (1). Nevertheless, at this stage, the existence of a catalytic mechanism in which the ribosome takes place cannot be excluded.

CONCLUDING REMARKS

Ribosomal crystallography, initiated two decades ago, yielded recently exciting structural and clinical information. The findings that the studied antibiotics interact almost exclusively with the RNA chains, explains why resistance to antibiotics that target ribosomes in clinical strains can be linked, in many cases, to mutations of the ribosomal RNA within functional relevant regions. As the therapeutic use of antibiotics has been severely hampered by the emergence of drug resistance in many pathogenic bacteria, revealing antibiotics binding sites may assist not only rational drug design but may also open the door for minimizing drug resistance. Still to be revealed is the high resolution structure of the entire ribosome and the mechanism of peptide bond formation. The recently identified mesophilic source, the ribosomes of which crystallize under close to physiological conditions, in unbound state as well as in complexes with

antibiotics or substrates, indicate that more excitements are due in the foreseeable future.

ACKNOWLEDGEMENTS

These studies were performed at the Structural Biology Department of the Weizmann Institute, the Max Planck Research Unit for Ribosomal Structure and in the Max-Planck Institute for Molecular Genetics in Berlin. Thanks are given J.M. Lehn for indispensable advice, R. Wimmer for recommending the ribosomal source, M. Wilchek, W. Traub, L. Shimon and A. Mankin for critical discussions. These studies could not be performed without the cooperation and assistance of the staff of the synchrotron radiation facilities at EMBL & MPG at DESY; ID14/2&4 at EMBL/ESRF and ID19/APS/ANL. The Max-Planck Society, the US National Institute of Health (GM34360), the German Ministry for Science and Technology (Bundesministerium für Bildung, Wissenschaft, Forschung und Technologie Grant 05-641EA) and the Kimmelman Center for Macromolecular Assembly at the Weizmann Institute provided support. AY holds the Martin S. Kimmel Professorial Chair.

REFERENCES

- [1] Yonath, A.; Mussig, J.; Tesche, B.; Lorenz, S.; Erdmann, V.; Wittmann, H.G. (1980) *Biochem. Internat.*, 1, 428, 31-35.
- [2] Yonath, A.; Bartunik, A.D.; Bartels, K.; Wittmann, H.G.; (1984) *J. Mol. Biol.*, 177, 201-6.
- [3] Shevack, A.; Gewitz, H.S.; Hennemann, B.; Yonath, A.; Wittmann, H.G. (1985) *FEBS lett.*, 184, 68-73.
- [4] Makowski, I.; Frolow, F.; Shoham, M.; Wittmann, H.G.; Yonath, A.; (1987) *J. Mol. Biol.*, 193, 819-22.
- [5] von Boehlen, K.; Makowski, I.; Hansen, H.A.; Bartels, H.; Berkovitch-Yellin, Z.; et al.; (1991) *J. Mol. Biol.*, 222, 11-15.
- [6] Yonath, A.; Glotz, C.; Gewitz, H.A. Bartels, K.S. von Bohlen, K. et al. (1988) *J. Mol. Biol.*, 203, 831-4.
- [7] Trakhanov, S.D.; Yusupov, M.M.; Agalarov, S.C.; Garber, M.B.; Ryazantsev, S.N.; et al. (1987) *FEBS Letters*, 220, 319-22.
- [8] Harms, J.; Schluenzen, F.; Zarivach, R.; Bashan, A.; Gat, S.; et al. (2001) *Cell*, in the press.
- [9] Hansen, H.A.S.; Volkmann, N.; Piefke, J.; Glotz, C.; Weinstein, S.; Makowski, I.; et al. (1990) *Biochim. Biophys. Acta*, 1050, 1-7.
- [10] Hope, H.; Frolow, F.; von Boehlen, K.; Makowski, I.; Kratky, C. et al. (1989) *Acta Cryst.*, B345, 190.
- [11] Ban, N.; Nissen, P.; Hansen, J.; Moore, P.B.; Steitz, T.A.; (2000) *Science*, 289, 905-20.
- [12] Schluenzen, F.; Tocilj, A.; Zarivach, R.; Harms, J.; Glühmann, M.; et al. (2000) *Cell*, 102, 615-23.
- [13] Wimberly, B.T.; Brodersen, D.E.; Clemons, W.M.; Jr, Morgan-Warren, R.J.; Carter, A.P.; et al. (2000) *Nature*, 407, 327-39.
- [14] Nissen, P.; Hansen, J.; Ban, N.; Moore, P.B.; Steitz, T.A. (2000) *Science*, 289, 920-30.
- [15] Brodersen, D.E.; Clemons, W.M.; Carter, A.P.; Morgan-Warren, R.J.; Wimberly, B.T.; et al. (2000) *Cell*, 103, 1143-54.
- [16] Carter, A.P.; Clemons, W.M.; Brodersen, D.E.; Morgan-Warren, R.J.; Wimberly, B.T.; et al. (2000) *Nature*, 407, 340-8.
- [17] Carter, A.P.; Clemons, W.M.; Jr, Brodersen, D.E.; Morgan-Warren, R.J.; Hartsch, T.; et al. (2001) *Science*, 291, 498-501.
- [18] Yusupov, M.M.; Yusupova, G.Z.; Baucom, A.; Lieberman, K.; Earnest, T.N.; et al. (2001) *Science*, 292, 883-96.
- [19] Ogle, J.M.; Brodersen, D.E.; Clemons, W.M.; Jr, Tarry, M.J.; et al (2000) *Science*, 292, 897-902.
- [20] Pioletti, M.; Schlunzen, F.; Harms, J.; Zarivach, R.; Gluhmann, M.; et al. (2001) *EMBO J.*, 20, 1829-39.
- [21] Schluenzen, F.; Zarivach, R.; Harms, J.; Bashan, A.; Tocilj, A.; et al. (2001) *Nature*, 413, 814-821.
- [22] Ginzburg, M.; Sacks, L.; Ginzburg, B.Z.; (1970) *J. Gen. Physiology*, 55, 178-207.
- [23] Harms, J.; Tocilj, A.; Levin, I.; Agmon, I.; Stark, H.; et al. (1999) *Structure Fold Des.*, 7, 931-941.
- [24] Yonath, A.; Harms, J.; Hansen, H.A.S.; Bashan, A.; Schlunzen, F.; et al. (1998) *Acta Cryst. A.*, 54, 945-55.
- [25] Ban, N.; Nissen, P.; Hansen, J.; Capel, M.; Moore, P.; Steitz, T.A.; (1999) *Nature*, 400, 841-847.
- [26] Weinstein, S.; Jahn, W.; Glotz, C.; Schluenzen, F.; Levin, I.; et al. (1999) *J. Struc. Biol.*, 127, 141-51.
- [27] Barta, A.; Dorner, S.; Polacek, N.; (2001) *Science*, 291, 203-4.
- [28] Bayfield, M.A.; Dahlberg, A.E.; Schulmeister, U.; Dorner, S. and Barta, A.; (2001) *Proc. Natl. Acad. Sci. USA*, 98, 10096-101.
- [29] Polacek, N.; Gaynor, M.; Yassin, A.; Mankin, A.S.; (2001) *Nature*, 411, 498-501.
- [30] Thompson, J.; Kim, D.F.; O'Connor, M.; Lieberman, K.R.; Bayfield, M.A.; et al. (2001) *Proc. Natl. Acad. Sci. USA*, 98, 9002-07.
- [31] Chandra Sanyal, S.; and Liljas, A.; (2000) *Curr. Opin. Struct. Biol.*, 10, 633-6.
- [32] Cundliffe, E.; Dixon, P.; Stark, M.; Stoffler, G.; Ehrlich, R.; et al. (1979) *J. Mol. Biol.*, 132, 235-52.
- [33] Nikonov, S.; Nevskaya, N.; Eliseikina, I.; Fomenkova, N.; Nikulin, A.; et al. (1996) *EMBO J.*, 15, 1350-9.
- [34] Subramanian, A.R. and Dabbs, E.R. (1980) *Eur. J. Biochem.*, 112, 425-30.

- [35] Wahl, M.C.; Bourenkov, G.P.; Bartunik, H.D. and Huber, R. (2000) *EMBO J.*, 19, 174-86.
- [36] Wimberly, B.T.; Guymon, R.; McCutcheon, J.P.; White, S.W.; and Ramakrishnan, V. (1999). *Cell*, 97, 491-502.
- [37] Franceschi, F.; Sagi, I.; Boeddeker, N.; Evers, U.; Arndt, E.; et al. (1994) *Syst. & App. Microbiology*, 16, 697-705.
- [38] Evers, U.; Franceschi, F.; Boeddeker, N.; Yonath, A. (1994) *Biophys. Chem.*, 50, 3-16.
- [39] White, O.; Eisen, J.A.; Heidelberg, J.F.; Hickey, E.K.; Peterson, J.D.; Dodson, R.J.; Haft, D.H.; Gwinn, M.L.; Nelson, W.C.; Richardson, D.L.; Moffat, K.S.; Qin, H.; Jiang, L.; Pamphile, W.; Crosby, M.; Shen, M.; Vamathevan, J.J.; Lam, P.; McDonald, L.; Utterback, T.; Zalewski, C.; Makarova, K.S.; Aravind, L.; Daly, M.J. and Fraser, C.M. (1999) *Science*, 286, 1571-7.
- [40] Porse, B.T. and Garrett, R.E.A. (1995) *J. Mol. Biol.*, 249, 1-10.
- [41] Hall, C.; Johnson, D. and Coppermann, B.S. (1988) *Biochemistry*, 27, 3983-3990.
- [42] Moazed, D.; and Noller, H.F. (1987) *Nature*, 327, 389-394.
- [43] Miskin, R.; Zamir, A. and Elson, D. (1968) *Biochem. Biophys. Res. Commun.*, 33, 551-557.
- [44] Vogel, Z.; Vogel, T.; Zamir, A. and Elson, D. (1971) *J. Mol. Biol.*, 60, 339-346.
- [45] Zamir, A.; Miskin, R.; Vogel, Z. and Elson, D. (1974) *Methods Enzymol.*, 30, 406-426.
- [46] Sonenberg, N.; Wilchek, M.; Zamir, A. (1973) *Proc. Natl. Acad. Sci. USA*, 70, 1423-26.
- [47] Wower, I.K.; Wower, J. and Zimmermann, R.A. (1998) *J. Biol. Chem.*, 273, 19847-52.
- [48] Bischof, O.; Urlaub, H.; Kruff, V. and Wittmann-Liebold, B. (1995) *J. Biol. Chem.*, 270, 23060-4.
- [49] Malkin, L.I. and Rich, A. (1967) *J. Mol. Biol.*, 26, 329-46.
- [50] Sabatini, D.D. and Blobel, G. (1970) *J. Cell Biol.*, 45, 146-57.
- [51] Milligan, R.A.; and Unwin, P.N. (1986) *Nature*, 319, 693-5.
- [52] Yonath, A.; Leonard, K.R.; and Wittmann, H.G. (1987) *Science*, 236, 813-6.
- [53] Fedorov, R.; Meshcheryakov, V.; Gongadze, G.; Fomenkova, N.; Nevskaya, N.; Selmer, M.; Laurberg, M.; Kristensen, O.; Al-Karadaghi, S.; Liljas, A.; Garber, M. and Nikonov, S. (2001) *Acta Cryst. D*, 57, 968-76.
- [54] Lu, M. and Steitz, T.A. (2000) *Proc. Natl. Acad. Sci. USA*, 97, 2023-8.
- [55] Agrawal, R.K.; Spahn, C.M.T.; Penczek, P.; Grassucci, R.A.; Nierhaus, K.H. and Frank, J. (2000) *J. Cell Biol.*, 150, 447-459.
- [56] Mueller, F.; Sommer, I.; Baranov, P.; Matadeen, R.; Stoldt, M.; J. Woehnert, M.; Goerlach, J.; van Heel, M. and Brimacombe, R. (2000) *J. Mol. Biol.*, 298, 35.
- [57] Ryan, P.C.; Lu, M. and Draper, D.E. (1991) *J. Mol. Biol.*, 221, 1257-68.
- [58] Hinck, A.P.; Markus, M.A.; Huang, S.; Grzesiek, S.; Kustonovich, I.; Draper, D.E. and Torchia, D.A. (1997) *J. Mol. Biol.*, 234, 1013-1020.
- [59] Conn, G.L.; Draper, D.E.; Lattman, E.E. and Gittis, A.G. (1999) *Science*, 284, 1171-1174.
- [60] GuhaThakurta, D. and Draper, D.E. (2000) *J. Mol. Biol.*, 295, 569-80.
- [61] Agrawal, R.K.; Linde, J.; Sengupta, J.; Nierhaus, K.H. and Frank, J. (2001) *J. Mol. Biol.*, 311, 777-787.
- [62] Nakashima, T.; Yao, M.; Kawamura, S.; Iwasaki, K.; Kimura, M. and Tanaka, I. (2001) *RNA*, 7, 692-701.
- [63] Walleczek, J.; Martin, T.; Redl, B.; Stoffler-Meilicke, M.; and Stoffler, G. (1989) *Biochemistry*, 28, 4099-105.
- [64] Mankin, A.S. and Garrett R.A. (1991) *J. Bacteriol.*, 173, 3559-63.
- [65] Tenson, T.; DeBlasio, A. and Mankin, A. (1996) *Proc. Natl. Acad. Sci. USA*, 93, 5641-5646.
- [66] Gregory, S.T. and Dahlberg, A.E. (1999) *J. Mol. Biol.*, 289, 827-834 Vazquez, D. (1975) *Inhibitors of protein synthesis* (Springer Verlag, Berlin, Germany).
- [67] Gabashvili, I.S.; Gregory, S.T.; Valle, M.; Grassucci, R.; Worbs, M.; Wahl, M.C.; Dahlberg, A.E. and Frank, J. (2001) *Mol. Cell*, 8, 181-188.
- [68] Vazquez, D. (1975) *Inhibitors of protein synthesis* (Springer Verlag, Berlin, Germany).
- [69] Kalliarafopoulos, S.; Kalpaxis, D.L. and Coutso-georgopoulos, C. (1994) *Mol. Pharmacol.*, 46, 1009-1014.